PHOTONICS Research

Hong–Ou–Mandel interference linking independent room-temperature quantum memories

Chao-Ni Zhang,[1,2,†] Hang Li,[1,2,†] Jian-Peng Dou,[1,2] Feng Lu,[1,2] Hong-Zhe Yang,[1,2] Xiao-Ling Pang,[1,2] and Xian-Min Jin[1,2,3,*]

[1]Center for Integrated Quantum Information Technologies (IQIT), School of Physics and Astronomy and State Key Laboratory of Advanced Optical Communication Systems and Networks, Shanghai Jiao Tong University, Shanghai 200240, China
[2]CAS Center for Excellence and Synergetic Innovation Center in Quantum Information and Quantum Physics, University of Science and Technology of China, Hefei 230026, China
[3]TuringQ Co., Ltd., Shanghai 200240, China
*Corresponding author: xianmin.jin@sjtu.edu.cn

Received 9 May 2022; revised 11 August 2022; accepted 13 August 2022; posted 16 August 2022 (Doc. ID 463404); published 29 September 2022

To realize a large-scale quantum network, both quantum memory and the interference of retrieved indistinguishable photons are essentially required to perform multi-photon synchronization and quantum-interference-mediated entanglement swapping. Significant progress has been achieved in low-temperature and well-isolated systems. However, linking independent quantum memories at room temperature remain challenging. Here, we present an experimental demonstration of Hong–Ou–Mandel interference between single photons from two independent room-temperature quantum memories. We manage to simultaneously operate two such quantum memories and individually obtain a memory-built-in quantum correlation of Stokes and anti-Stokes photons by a far-off-resonance Duan–Lukin–Cirac–Zoller protocol. We also successfully enhance the Hong–Ou–Mandel interference rate up to about 15 times by increasing each photon rate, which is achieved by coordinating two quantum memories with a repeat-until-success fashion. We observe the visibility of quantum interference up to 75.0% without reduction of any background noise, well exceeding the classical limit of 50%. Our results, together with its straightforward, broadband, and room-temperature features, open up a promising way towards realizing large-scale quantum networks at ambient conditions.

https://doi.org/10.1364/PRJ.463404

1. INTRODUCTION

Distributing quantum entanglement between remote nodes is one of the fundamental primitives for quantum information processing, such as quantum communication [1–4], distributed quantum computing [5–7], and quantum teleportation [8–10]. Direct transmission of qubits seems to be a straightforward strategy. However, due to the increasing photon loss and noise in the channel [11,12], it is attainable just within a moderate distance. A promising solution is the quantum repeater scheme, where entanglements are preliminarily generated between intermediate nodes within the attenuation length and then extended via linking the adjacent segments [13]. This hierarchical architecture shifts the experimental focus from reducing transmission loss into overcoming the probabilistic generation of the entanglement for each segment. It necessitates the nodes functioning as quantum memories, and therefore the generated entanglement can be kept for waiting for the other to be accomplished [14–16].

Besides, connecting entangled segments is usually mediated by photons retrieved from neighboring nodes [17–19]. While two photons are respectively correlated with the internal state of the remaining nodes, their interference validates operations like Bell state measurement to project the matter systems into an entangled state. An essential requirement in this optical scheme is the indistinguishability of photons from different repeater nodes, which can be demonstrated by the Hong–Ou–Mandel (HOM) interference [20,21].

So far, HOM interference between photons retrieved from two single-photon sources has been realized in various systems, such as cold atomic ensembles [22,23], single atoms [24], nitrogen vacancy centers [25,26], and trapped ions [27]. To avoid noise and decoherence from atomic thermal motion, these systems are mostly operated at cryogenic temperatures and in well-isolated environments [28,29]. Recent progress has shown interest in room-temperature systems [30,31], which offer better scalability as they are free from the complex cooling apparatus.

Quantum interference between two single photons from the spontaneous four-wave mixing (SFWM) process in room-temperature atomic ensembles has been reported [30]. It obtains high interference visibility but does not operate on demand. Recently, the far off-resonance Duan–Lukin–Cirac–Zoller (DLCZ) protocol demonstrates the feasibility of combining single-photon generation with memory capability in a room-temperature system [32–34]. This DLCZ-type source prototypes repeater nodes in the pioneering proposal [17] for quantum networks, and the far-off-resonance configuration endows extra broadband feature for high operation rate. But for further application, proving the ability of generating indistinguishable photons from independent sources remains to be proved.

In this work, we prepare two individual single-photon sources based on quantum memories, operating in a heralded, low-noise, and broadband fashion. The memory-built-in feature of our ensemble-based source enables a repeat-until-success strategy in the single-photon generation, thereby speeding up the process of HOM interference, representing a promising way towards realizing large-scale quantum networks at ambient conditions.

2. EXPERIMENTAL SETUP

We perform the experiment on two vapor cells containing cesium atoms, each acting as a memory-built-in single-photon source. Figure 1(a) shows the Λ-type atomic configuration employed for the single-photon generation, consisting of a ground state $|g\rangle$ for initialization, another ground state $|s\rangle$ for storing excitation, and an excited state labeled $|e\rangle$. For each trial, all atoms are initially prepared in the ground state $|g\rangle$ via a pump light resonant with $|s\rangle \rightarrow |e\rangle$ transition. Afterward, a collective excitation is created via spontaneous Raman scattering, which is heralded by the accompanying Stokes photon. After a programmable delay, the stored collective excitation can be mapped into a single photon by applying a read pulse [35,36]. Notably, a large detuning is applied (13.2 GHz in the write process and 4 GHz in the read process, respectively) to avoid the fluorescence noise in room-temperature ensembles. Making use of the orthogonal polarization, the signal photons are separated from the strong control light via a high-extinction-ratio Wollaston prism. They are further purified by a cascaded Fabry–Perot cavity, which also serves as a splitter to transmit Stokes photons and anti-Stokes photons into different paths. Finally, the heralded anti-Stokes photons from two independent sources are respectively collected by single-mode fibers and directed into a fiber beam splitter for HOM interference. More experimental details can be found in Appendix A.

In an ideal case, the indistinguishability between two incident photons governs this completely destructive two-photon interference [20]; while in practice, the multi-photon component of the photon sources also contributes to the coincidental events at outputs of the fiber beam splitter and therefore leads to a reduction of interference visibility. For the purpose of suppressing the multi-photon component, the ensemble-based source applies a weak pulse in the write process to reduce the creation of high-order excitation [36]. However, this causes a limited single-photon generation rate for the interference experiment.

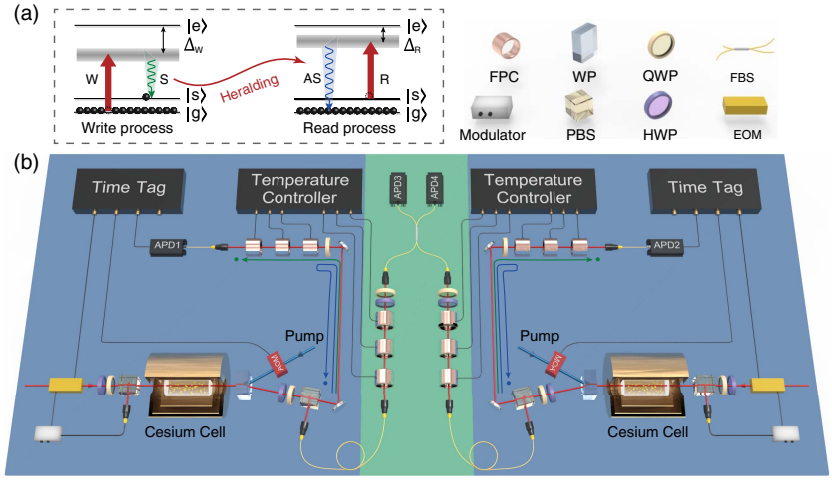

Fig. 1. Schematic view of the experiment. (a) The atomic energy level of ^{133}Cs for generating heralded single photons, with $|g\rangle = |6S_{1/2}, F = 3\rangle$, $|s\rangle = |6S_{1/2}, F = 4\rangle$, and the excited state $|e\rangle$ representing the manifold of the $6P_{3/2}$ state. (b) The experimental setup. To generate the write and read pulses, an electro-optical modulator is utilized to chop the continuous laser into a pulse sequence. An automatic feedback circuit monitors and locks the operating point of the electro-optical modulator, achieving stable operation over the long term. According to the response of the detector in the Stokes channel, the time tag module varies the drive electric signal of the electro-optical modulator, implementing conditional control of single-photon generation. The Stokes photon and anti-Stokes photon are co-propagating in the coaxial write-read scheme. To separate the Stokes photons and anti-Stokes photons into different paths, we placed a 45° oriented quarter-wave plate in front of the Stokes-resonant cavity, rotating both photons into right circular polarization. The Stokes photons go through the cavity while the anti-Stokes photons are reflected by this cavity at its front surface, and then pass the quarter-wave plate again. This makes the anti-Stokes photons vertically polarized, which enables the anti-Stokes photons to be reflected by the PBS and finally directed to the anti-Stokes-resonant cavity. Stokes photons are detected by APD1 and APD2, while anti-Stokes photons are detected by APD3 and APD4. FPC, Fabry–Perot cavity; WP, Wollaston prism; QWP, quarter-wave plate; FBS, fiber beam splitter; PBS, polarization beam splitter; HWP, half-wave plate; EOM, electro-optical modulator; and APD, avalanche photodiode.

To speed up the process of obtaining the HOM dip, a repeat-until-success protocol is introduced to enhance the generation rate of heralded single photons. For each source, N write pulses with an equal interval are applied to the ensembles, repeating the write process until a Stokes photon is detected [23,37]. As two sources are mutually independently manipulated, one can continue to repeat the write process while the other one successfully stores the generated collective excitation. When the collective excitations are prepared in both atomic ensembles, read pulses at a pre-determined moment are applied to both ensembles to obtain the anti-Stokes photons simultaneously. Otherwise, the repeat-until-success write process also stops when the maximum number of write pulses has been reached.

3. RESULTS

Obviously, the ability to preserve the generated collective excitation is a key factor for this protocol. It is quantified by measuring the cross-correlation function between the Stokes photons and the anti-Stokes photons (see Fig. 2), which implies that the generated collective excitation can be preserved for an on-demand memory time [37,38]. To realize the repeat-until-success protocol, four write pulses are pre-programmed in each period and the output of the detector of the Stokes photon is transmitted into the pulse generation system. Upon detecting a Stokes photon, the signal from this detector triggers the pulse generation system to stop generating the subsequent write pulses. Otherwise, it works as pre-determined. Here, the time interval between adjacent write pulses is 125 ns, a litter bit longer than a single period of detection and feedback. In this case, the repeat-until-success protocol enables a 3.8 times enhancement of generation rate for each photon source and then about 15 times increase in the probability of simultaneously obtaining heralded single photons from two independent quantum memories.

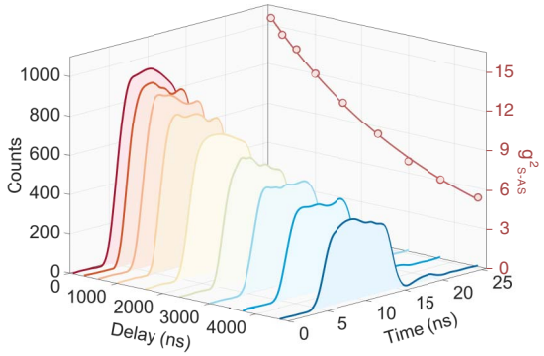

Fig. 2. Heralded single photon with a different time delay in quantum memory. The solid curves in the main part refer to the temporal shape of the generated single photon with a different time delay for retrieval, without reduction of any background noise. The red dots on the right side denote the corresponding cross-correlation function between the Stokes and anti-Stokes photons.

In addition, it is also accessible to manipulate the rate of four-fold coincidence by changing the power of the control light. As shown in Fig. 1, to adjust the power of the control pulse, a combination of a half-wave plate and a quarter-wave plate is placed in front of the polarization beam splitter, controlling the ratio of light incident into the ensemble. Figure 3(a) shows the counts of the heralded single photon increasing with the energy of the write pulse. It indicates that a strong control pulse is required for a high rate of four-fold events. But, on the other hand, when applying a stronger control pulse, both high-order excitation in the write process and the four-wave mixing process in the read process are strengthened [17,33]. Along with the energy-dependent leaking from the control pulses, the increased noise degrades the fidelity of the generated single photon and thereby results in a lower interference visibility. We analyze the photon statistic property via a Hanbury Brown–Twiss interferometer, and the single-photon character is quantified by an anti-correlation parameter [39,40]. For the chosen energy of 330 pJ per write pulse, the measured four-fold coincidence rate is about 20 events/h, and the anti-correlation parameter of the single-photon source is 0.326 ± 0.024, therefore leading to a good trade-off between the rate of four-fold coincidence and the interference visibility.

To observe high-visibility HOM interference, the properties of the relative photons here are carefully engineered to be

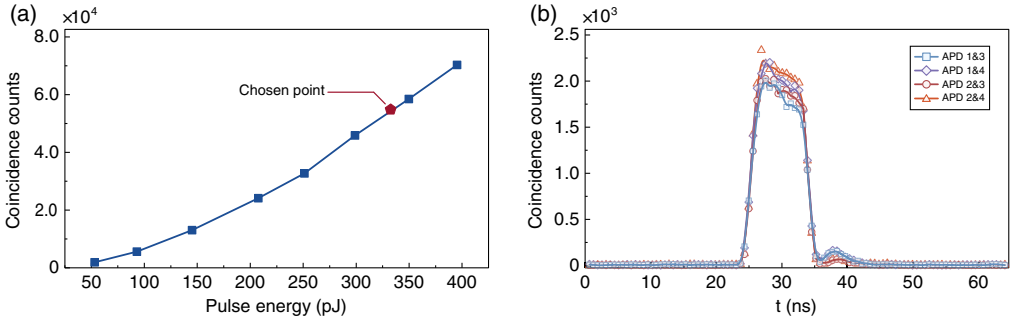

Fig. 3. Characterization of the two single-photon sources from independent room-temperature quantum memories. (a) The counts of the heralded anti-Stokes photons as a function of the write pulse power with 566,037,735 trials performed. The red pentagon refers to the chosen pulse energy in this experiment. (b) The temporal shape of the heralded anti-Stokes photons generated by two photon sources. The blue squares (purple rhombuses) mark the heralded anti-Stokes photons from one photon source detected by APD3 (APD4), while the red dots (orange triangles) represent the heralded anti-Stokes photons that are generated by another photon source and detected by APD3 (APD4). These data are obtained with a pulse energy of 330 pJ and 566,037,735 repeated trials.

indistinguishable [24,25]. After coupling into single-mode fibers, the anti-Stokes photons from two independent sources are both in the transverse Gaussian mode. Different from the condition with the bulk beam splitter, a good spatial overlap is easily achieved when two incident photons are mixed in a fiber beam splitter. For the polarization degree of freedom, the anti-Stokes photons are both vertically polarized after being separated from the strong read pulse via a high-extinction-ratio Wollaston prism. But their polarization is dissimilarly rotated by fibers and other optical devices during the propagation. We then adjust the half-wave plates and quarter-wave plates, which are positioned at the input ports of the single-mode fibers, to compensate for this polarization difference before they superpose on the fiber beam splitter. In addition, the energy, the spatial profile, and the duration of the control pulse are finely tuned to match the temporal mode of the photons [41]. Figure 3(b) shows the measured temporal shapes of the anti-Stokes photons from two sources, indicating high similarity between them.

For an HOM interference experiment in the time domain, the time interval between two heralded anti-Stokes photons is changed from overlap to separation [23]. We introduce this time delay by varying the time interval between two electric control signal sequences, which are respectively applied to drive two pulse generation systems. Figure 4 shows the registered four-fold coincidence counts as a function of the arrival time difference for two independent anti-Stokes photons, where the time step is 3.75 ns. The solid curve is the theoretical result based on the parameters in our experiment [42,43]. Without subtracting the accidental coincidence from the background noise and the detector dark counts, the result gives a visibility of $(75.0 \pm 5.1)\%$. The obtained visibility exceeds the classical limit of 50%, indicating the non-classical property of two anti-Stokes photons and the indistinguishability between them [22,30].

To further investigate the nonideal interference at zero delay, we analyze our result with the model from Ref. [44]. In this model, the nonvanishing dip is attributed to the imperfect indistinguishability between two photons and multi-photon component of the photon sources [44,45]. In our experiment, the measured anti-correlation parameters of the single-photon sources are 0.323 ± 0.023 and 0.326 ± 0.024, respectively. According to the model in Ref. [44], these multi-photon components reduce the achievable visibility to $(75.6 \pm 5.1)\%$. The estimated value is quite close to the measured one, leaving a small residual reduction of visibility caused by the distinguishability between photons. At present, this indicates that the single-photon purity of the sources is the dominant factor for visibility degradation. Therefore, efforts for improving the single-photon purity, like adding clear pump pulses between adjacent write pulses and suitably decreasing the energy of the control pulses, will significantly enhance the interference visibility.

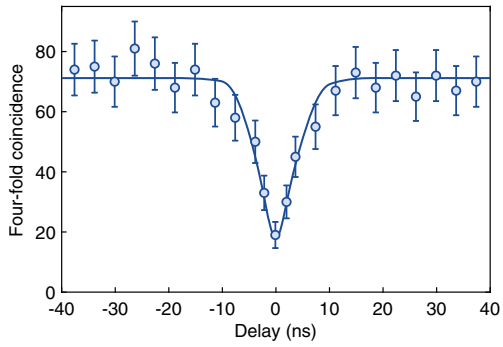

Fig. 4. Four-fold coincidence as a function of the time delay between two photons from independent room-temperature quantum memories. The blue dots correspond to the experimental data with an effective measurement of 11,886,792,452 trials, and the solid line represents the theoretical curve. The error bars denote one standard deviation.

4. CONCLUSIONS AND DISCUSSION

In summary, we have successfully demonstrated HOM interference between heralded single photons from two independent room-temperature quantum memories. The measured interference visibility shows the capability of such independent sources for constructing a quantum memory-enabled network. Its further analysis highlights the potential improvement by suppressing the multi-photon component, e.g., by elaborating the cavity engineering to reduce four-wave-mixing noise [46] or adding clear pump pulses between write pulses to reinitialize the state of the atomic ensemble [23]. Along with the achieved near-millisecond lifetime [33], our result certifies the feasibility for engineering, manipulating, and transferring quantum resources with room-temperature quantum memories, and the realization of long-distance quantum communication and optical quantum computing at ambient conditions.

APPENDIX A: EXPERIMENTAL DETAILS

As shown in the Fig. 1 in the main text, a 75-mm-long cesium vapor cell with 10 Torr Ne buffer gas is employed for each quantum memory. The vapor cell is packed in a three-layer magnetic shielding, and its temperature is stabilized at 61°C for a large optical depth of about 5000. In each trial, the pump, write, and read pulses are applied on the atomic ensemble to generate the heralded single photons. The pump pulse is generated by an external cavity diode laser, resonant with the transition $6S_{1/2}, F = 4 \rightarrow 6P_{3/2}, F' = 4$ co 5 crossover of ^{133}Cs. Controlled by an acousto-optic modulator, the pump light is turned on for 480 ns at the beginning of each trial, preparing all atoms in the ground state. Both write pulses and read pulses are provided by another distributed Bragg reflector (DBR) laser. Comparing with the pump light, the frequency of the DBR laser is red detuned by 4 GHz to minimize the fluorescence noise. Appropriate electric signals are applied on the fast electro-optical modulator to chop the continuous laser into desired write pulses or read pulses. The energy of the generated pulses is first amplified by a homemade tapered amplifier and then finely tuned via controlling the polarization of the pulses before these pulses pass a polarization beam splitter. In our system, the beam waist of both the write pulse and the read pulse is about 391.0 μm in the vapor cell. The energy of the write pulse and read pulse is 330 pJ and 740.9 pJ, respectively.

Signal photons with vertical polarization and control pulses with horizontal polarization are separated by a Wollaston

Table 1. Characteristics of the Single-Photon Source and Measured Four-Fold Coincidence Rate

Parameter	Value
Counting rate of Stokes photon	$5.9 \times 10^3\ s^{-1}$
Counting rate of the heralded anti-Stokes photon	$90.3\ s^{-1}$
Anti-correlation parameter	0.326 ± 0.024
Four-fold coincidence rate	$20.3\ h^{-1}$

prism. Due to the non-negligible noise from the leakage of the control pulses, further purification is needed for a higher signal-to-noise ratio. Therefore, the Stokes photons and anti-Stokes photons are collected into a single-mode fiber and transmitted to frequency filters (cascaded cavities) to filter out the residual control pulses. The measured peak transmission of the single cavity reaches 90%, and a high extinction ratio of about 10^7 is obtained after Stokes (anti-Stokes) photons pass three cascaded resonant cavities. After leaving the cavity, the purified Stokes photons and anti-Stokes photons are detected by single-photon detectors, providing information about the properties of the single-photon sources. For the chosen energy of write pulse, the measured probability of detecting a Stokes photon in a trial is about 6.24×10^{-3} by utilizing the repeat-until-success protocol. Conditioned on the detection of a Stokes photon, the probability of detecting an anti-Stokes photon is about 1.53%. Notably, the above parameters are obtained by analyzing the recorded photon counts, where loss from coupling, filtering, and inefficient detection has been included. For the propagation from the atomic ensemble to the detector, the transmission efficiency of the fiber coupling and the filter together is about 17.3% in the Stokes channel and 16.5% in the anti-Stokes channel. The quantum efficiency of the detector is about 50%. For clarity, some important experimental parameters are shown in Table 1.

Funding. National Key Research and Development Program of China (2019YFA0706302, 2019YFA0308700, 2017YFA0303700); National Natural Science Foundation of China (NSFC) (11904229, 61734005, 11761141014, 11690033); Science and Technology Commission of Shanghai Municipality (STCSM) (20JC1416300, 2019SHZDZX01); Shanghai Municipal Education Commission (SMEC) (2017-01-07-00-02-E00049); China Postdoctoral Science Foundation (2020M671091); Shanghai Talent Program; Zhiyuan Innovative Research Center of Shanghai Jiao Tong University.

Acknowledgment. The authors thank Jian-Wei Pan for helpful discussions. X.-M. J. acknowledges additional support from a Shanghai talent program and support from the Zhiyuan Innovative Research Center of Shanghai Jiao Tong University.

Disclosures. The authors declare no conflicts of interest.

Data Availability. Data underlying the results presented in this paper are not publicly available at this time but may be obtained from the authors upon reasonable request.

†These authors contributed equally to this paper.

REFERENCES

1. P. Zoller, T. Beth, D. Binosi, R. Blatt, H. Briegel, D. Bruss, T. Calarco, J. I. Cirac, D. Deutsch, J. Eisert, A. Ekert, C. Fabre, N. Gisin, P. Grangiere, M. Grassl, S. Haroche, A. Imamoglu, A. Karlson, J. Kempe, L. Kouwenhoven, S. Kröll, G. Leuchs, M. Lewenstein, D. Loss, N. Lütkenhaus, S. Massar, J. E. Mooij, M. B. Plenio, E. Polzik, S. Popescu, G. Rempe, A. Sergienko, D. Suter, J. Twamley, G. Wendin, R. Werner, A. Winter, J. Wrachtrup, and A. Zeilinger, "Quantum information processing and communication: strategic report on current status, visions and goals for research in Europe," Eur. Phys. J. D **36**, 203–228 (2005).
2. S. Nauerth, F. Moll, M. Rau, C. Fuchs, J. Horwath, S. Frick, and H. Weinfurter, "Air-to-ground quantum communication," Nat. Photonics **7**, 382–386 (2013).
3. A. K. Ekert, "Quantum cryptography based on Bell's theorem," Phys. Rev. Lett. **67**, 661–663 (1991).
4. N. Gisin and R. Thew, "Quantum communication," Nat. Photonics **1**, 165–171 (2007).
5. J. I. Cirac, A. K. Ekert, S. F. Huelga, and C. Macchiavello, "Distributed quantum computation over noisy channels," Phys. Rev. A **59**, 4249–4254 (1999).
6. J. Preskill, "Quantum computing in the NISQ era and beyond," Quantum **2**, 79 (2018).
7. A. Steane, "Quantum computing," Rep. Prog. Phys. **61**, 117–173 (1998).
8. D. Bouwmeester, J.-W. Pan, K. Mattle, M. Eibl, H. Weinfurter, and A. Zeilinger, "Experimental quantum teleportation," Nature **390**, 575–579 (1997).
9. A. Furusawa, J. L. Sørensen, S. L. Braunstein, C. A. Fuchs, H. J. Kimble, and E. S. Polzik, "Unconditional quantum teleportation," Science **282**, 706–709 (1998).
10. S. Pirandola, J. Eisert, C. Weedbrook, A. Furusawa, and S. L. Braunstein, "Advances in quantum teleportation," Nat. Photonics **9**, 641–652 (2015).
11. J. F. Dynes, H. Takesue, Z. L. Yuan, A. W. Sharpe, K. Harada, T. Honjo, H. Kamada, O. Tadanaga, Y. Nishida, M. Asobe, and A. J. Shields, "Efficient entanglement distribution over 200 kilometers," Opt. Express **17**, 11440–11449 (2009).
12. T. Inagaki, N. Matsuda, O. Tadanaga, M. Asobe, and H. Takesue, "Entanglement distribution over 300 km of fiber," Opt. Express **21**, 23241–23249 (2013).
13. H.-J. Briegel, W. Dür, J. I. Cirac, and P. Zoller, "Quantum repeaters: the role of imperfect local operations in quantum communication," Phys. Rev. Lett. **81**, 5932–5935 (1998).
14. Y.-F. Pu, S. Zhang, Y.-K. Wu, N. Jiang, W. Chang, C. Li, and L.-M. Duan, "Experimental demonstration of memory-enhanced scaling for entanglement connection of quantum repeater segments," Nat. Photonics **15**, 374–378 (2021).
15. C.-W. Chou, J. Laurat, H. Deng, K. S. Choi, H. de Riedmatten, D. Felinto, and H. J. Kimble, "Functional quantum nodes for entanglement distribution over scalable quantum networks," Science **316**, 1316–1320 (2007).
16. A. I. Lvovsky, B. C. Sanders, and W. Tittel, "Optical quantum memory," Nat. Photonics **3**, 706–714 (2009).
17. L.-M. Duan, M. D. Lukin, J. I. Cirac, and P. Zoller, "Long-distance quantum communication with atomic ensembles and linear optics," Nature **414**, 413–418 (2001).
18. Z.-B. Chen, B. Zhao, Y.-A. Chen, J. Schmiedmayer, and J.-W. Pan, "Fault-tolerant quantum repeater with atomic ensembles and linear optics," Phys. Rev. A **76**, 022329 (2007).
19. B. Zhao, Z.-B. Chen, Y.-A. Chen, J. Schmiedmayer, and J.-W. Pan, "Robust creation of entanglement between remote memory qubits," Phys. Rev. Lett. **98**, 240502 (2007).
20. C. K. Hong, Z. Y. Ou, and L. Mandel, "Measurement of subpicosecond time intervals between two photons by interference," Phys. Rev. Lett. **59**, 2044–2046 (1987).
21. C. Santori, D. Fattal, J. Vuckovic, G. S. Solomon, and Y. Yamamoto, "Indistinguishable photons from a single-photon device," Nature **419**, 594–597 (2002).
22. D. Felinto, C. W. Chou, J. Laurat, E. W. Schomburg, H. de Riedmatten, and H. J. Kimble, "Conditional control of the quantum

states of remote atomic memories for quantum networking," Nat. Phys. **2**, 844–848 (2006).
23. Z.-S. Yuan, Y.-A. Chen, S. Chen, B. Zhao, M. Koch, T. Strassel, Y. Zhao, G.-J. Zhu, J. Schmiedmayer, and J.-W. Pan, "Synchronized independent narrow-band single photons and efficient generation of photonic entanglement," Phys. Rev. Lett. **98**, 180503 (2007).
24. J. Beugnon, M. P. A. Jones, J. Dingjan, B. Darquié, G. Messin, A. Browaeys, and P. Grangier, "Quantum interference between two single photons emitted by independently trapped atoms," Nature **440**, 779–782 (2006).
25. A. Sipahigil, M. L. Goldman, E. Togan, Y. Chu, M. Markham, D. J. Twitchen, A. S. Zibrov, A. Kubanek, and M. D. Lukin, "Quantum interference of single photons from remote nitrogen-vacancy centers in diamond," Phys. Rev. Lett. **108**, 143601 (2012).
26. H. Bernien, L. Childress, L. Robledo, M. Markham, D. Twitchen, and R. Hanson, "Two-photon quantum interference from separate nitrogen vacancy centers in diamond," Phys. Rev. Lett. **108**, 043604 (2012).
27. P. Maunz, D. L. Moehring, S. Olmschenk, K. C. Younge, D. N. Matsukevich, and C. Monroe, "Quantum interference of photon pairs from two remote trapped atomic ions," Nat. Phys. **3**, 538–541 (2007).
28. K. C. Lee, M. R. Sprague, B. J. Sussman, J. Nunn, N. K. Langford, X.-M. Jin, T. Champion, P. Michelberger, K. F. Reim, D. England, D. Jaksch, and I. A. Walmsley, "Entangling macroscopic diamonds at room temperature," Science **334**, 1253–1256 (2011).
29. S. Manz, T. Fernholz, J. Schmiedmayer, and J.-W. Pan, "Collisional decoherence during writing and reading quantum states," Phys. Rev. A **75**, 040101 (2007).
30. T. Jeong, Y.-S. Lee, J. Park, H. Kim, and H. S. Moon, "Quantum interference between autonomous single-photon sources from Doppler-broadened atomic ensembles," Optica **4**, 1167–1170 (2017).
31. M. Flament, S. Gera, Y. Kim, A. Scriminich, M. Namazi, S. Sagona-Stophel, G. Vallone, P. Villoresi, and E. Figueroa, "Hong–Ou–Mandel interference of polarization qubits stored in independent room-temperature quantum memories," arXiv:1808.07015 (2019).
32. J.-P. Dou, A.-L. Yang, M.-Y. Du, D. Lao, J. Gao, L.-F. Qiao, H. Li, X.-L. Pang, Z. Feng, H. Tang, and X.-M. Jin, "A broadband DLCZ quantum memory in room-temperature atoms," Commun. Phys. **1**, 55 (2018).
33. K. B. Dideriksen, R. Schmieg, M. Zugenmaier, and E. S. Polzik, "Room-temperature single-photon source with near-millisecond built-in memory," Nat. Commun. **12**, 3699 (2021).
34. T.-H. Yang, C.-N. Zhang, J.-P. Dou, X.-L. Pang, H. Li, W.-H. Zhou, Y.-J. Chang, and X.-M. Jin, "Time-bin entanglement built in room-temperature quantum memory," Phys. Rev. A **103**, 062403 (2021).
35. N. Sangouard, C. Simon, H. de Riedmatten, and N. Gisin, "Quantum repeaters based on atomic ensembles and linear optics," Rev. Mod. Phys. **83**, 33–80 (2011).
36. S. Chen, Y.-A. Chen, B. Zhao, Z.-S. Yuan, J. Schmiedmayer, and J.-W. Pan, "Demonstration of a stable atom-photon entanglement source for quantum repeaters," Phys. Rev. Lett. **99**, 180505 (2007).
37. S. Chen, Y.-A. Chen, T. Strassel, Z.-S. Yuan, B. Zhao, J. Schmiedmayer, and J.-W. Pan, "Deterministic and storable single-photon source based on a quantum memory," Phys. Rev. Lett. **97**, 173004 (2006).
38. A. Kuhn, M. Hennrich, and G. Rempe, "Deterministic single-photon source for distributed quantum networking," Phys. Rev. Lett. **89**, 067901 (2002).
39. M. D. Eisaman, J. Fan, A. Migdall, and S. V. Polyakov, "Invited review article: single-photon sources and detectors," Rev. Sci. Instrum. **82**, 071101 (2011).
40. A. B. U'Ren, C. Silberhorn, J. L. Ball, K. Banaszek, and I. A. Walmsley, "Characterization of the nonclassical nature of conditionally prepared single photons," Phys. Rev. A **72**, 021802 (2005).
41. M. Dabrowski, R. Chrapkiewicz, and W. Wasilewski, "Hamiltonian design in readout from room-temperature Raman atomic memory," Opt. Express **22**, 26076–26091 (2014).
42. T. Legero, T. Wilk, A. Kuhn, and G. Rempe, "Time-resolved two-photon quantum interference," Appl. Phys. B **77**, 797–802 (2003).
43. Y.-H. Deng, H. Wang, X. Ding, Z.-C. Duan, J. Qin, M.-C. Chen, Y. He, Y.-M. He, J.-P. Li, Y.-H. Li, L.-C. Peng, E. S. Matekole, T. Byrnes, C. Schneider, M. Kamp, D.-W. Wang, J. P. Dowling, S. Höfling, C.-Y. Lu, M. O. Scully, and J.-W. Pan, "Quantum interference between light sources separated by 150 million kilometers," Phys. Rev. Lett. **123**, 080401 (2019).
44. A. N. Craddock, J. Hannegan, D. P. Ornelas-Huerta, J. D. Siverns, A. J. Hachtel, E. A. Goldschmidt, J. V. Porto, Q. Quraishi, and S. L. Rolston, "Quantum interference between photons from an atomic ensemble and a remote atomic ion," Phys. Rev. Lett. **123**, 213601 (2019).
45. R.-B. Jin, K. Wakui, R. Shimizu, H. Benichi, S. Miki, T. Yamashita, H. Terai, Z. Wang, M. Fujiwara, and M. Sasaki, "Nonclassical interference between independent intrinsically pure single photons at telecommunication wavelength," Phys. Rev. A **87**, 063801 (2013).
46. D. J. Saunders, J. H. D. Munns, T. F. M. Champion, C. Qiu, K. T. Kaczmarek, E. Poem, P. M. Ledingham, I. A. Walmsley, and J. Nunn, "Cavity-enhanced room-temperature broadband Raman memory," Phys. Rev. Lett. **116**, 090501 (2016).